Note added in proof: Similar conclusions were reached by Lin *et al.*[29] studying the association of APL fusion proteins and SMRT. □

Methods

Mutants, constructs and cell lines. PML–RARα and PLZF–RARα AHT mutants[19] were generated by the polymerase chain reaction (PCR) and subcloned in the pGMT-SV-NEO and pCDNA3 eukaryotic expression vectors. Stable U937 transfectants of PML–RARα, PML–RARα AHT and PLZF–RARα cloned into pGMT-SV-NEO were obtained by electroporation. The used PLZF mutants were generated by PCR and cloned within the pCDNA3 vector.

***In vitro* binding assays with GST fusion proteins.** The GST–N-CoR constructs 4–12 have been described previously[25]. Constructs 1–3 were generated by PCR and cloned in the pGex4T-1 vector. GST beads containing the fusion proteins (10 μg) were incubated in E1A buffer (50 mM HEPES, pH 7.8, 50 mM NaCl, 5 mM EDTA, 1 mM DTT, 0.1% NP40) with 5 μl of *in vitro*-translated polypeptides. After washing, bound proteins were eluted by boiling in SDS–PAGE loading buffer, resolved by electrophoresis, and visualized by autoradiography.

Co-immunoprecipitation experiments and western blotting analysis. Nuclear extracts were prepared as described[26]. Where indicated, RA (20 μM) was added 1 h before incubation of the nuclear extracts with the appropriate antibodies or controls. Immunocomplexes were recovered by protein A-Agarose beads and resolved by electrophoresis. Anti-N-CoR antiserum was raised against the GST–N-CoR 1–224.

Histone deacetylase assay. Assays for histone deacetylase activity were performed as described[27]. Immunoprecipitated complexes on protein A-agarose beads were incubated at 30 °C for 1 h with [^{3}H]acetate-labelled chicken erythrocyte histones. The reaction was stopped by addition of 0.7-vol of 1M HCl–0.4 M acetate. Released [^{3}H] acetic acid was extracted with ethyl acetate and quantified by liquid scintillation analysis. As a positive control, we measured histone deacetylase activity in anti-histone deacetylase-1 immunocomplexes.

Received 28 October; accepted 18 December 1997.

1. Grignani, F. *et al*. Acute promyelocytic leukaemia: from genetics to treatment. *Blood* **83,** 10–25 (1994).
2. Warrell, R. P. J., de Thé, H., Wang, Z. Y. & Degos, L. Acute promyelocytic leukaemia. *N. Engl. J. Med.* **324,** 177–189 (1993).
3. de The, H. *et al*. The PML-RAR alpha fusion mRNA generated by the t(15;17) translocation in acute promyelocytic leukemia encodes a functionally altered RAR. *Cell* **66,** 675–684 (1991).
4. Kakizuka, A. *et al*. Chromosomal translocation t(15;17) in human acute promyelocytic leukemia fuses RAR alpha with a novel putative transcription factor, PML. *Cell* **66,** 663–674 (1991).
5. Pandolfi, P. P. *et al*. Genomic variability and alternative splicing generate multiple PML/RAR alpha transcripts that encode aberrant PML proteins and PML/RAR alpha isoforms in acute promyelocytic leukaemia. *EMBO J.* **11,** 1397–1407 (1992).
6. Chen, Z. *et al*. Fusion between a novel Krüppel-like zinc finger gene and retinoic acid receptor-α locus due to a variant t(11;17) translocation associated with acute promyelocytic leukaemia. *EMBO J.* **12,** 1161–1167 (1993).
7. Chen, Z. *et al*. PLZF-RAR alpha fusion proteins generated from the variant t(11;17)(q23;q21) translocation in acute promyelocytic leukemia inhibit ligand-dependent transactivation of wild-type retinoic acid recetors. *Proc. Natl Acad. Sci. USA* **91,** 1178–1182 (1994).
8. Ruthardt, M. *et al*. Opposite effects of the Acute Promyelocytic Leukaemia PML/RARα and PLZF/RARα fusion proteins on retinoic acid signalling. *Mol. Cell. Biol.* **17,** 4859–4869 (1997).
9. Heinzel, T. *et al*. A complex containing N-CoR, mSin3 and histone deacetylase mediates transcriptional repression. *Nature* **387,** 43–49 (1997).
10. Nagy, L. *et al*. Nuclear receptor repression mediated by a complex containing SMRT, ,mSin3A, and histone deacetylase. *Cell* **89,** 373–380 (1997).
11. Grunstein, M. Histone acetylation in chromatin structure and transcription. *Nature* **389,** 349–352 (1997).
12. Wolffe, A. P. Sinful repression. *Nature* **387,** 16–17 (1997).
13. Mangelsdorf, D. J. & Evans, R. M. The RXR heterodimers and orphan receptors. *Cell* **83,** 841–850 (1995).
14. Minucci, S. & Ozato, K. Retinoid receptors in transcriptional regulation. *Curr. Opin. Genet. Dev.* **6,** 567–574 (1996).
15. Chambon, P. A decade of molecular biology of retinoid receptors. *FASEB J.* **10,** 940–954 (1996).
16. Hong, S., David, G., Wong, C., Dejean, A. & Privalsky, M. SMRT corepressor interacts with PLZF and with the PML-retinoic acid receptor alpha and PLZF-RAR alpha oncoproteins associated with acute promyelocytic leukaemia. *Proc. Natl Acad. Sci. USA* **94,** 9028–9033 (1997).
17. Grignani, F. *et al*. The acute promyelocytic leukemia-specific PML-RAR alpha fusion protein inhibits differentiation and promotes survival of myeloid precursor cells. *Cell* **74,** 423–431 (1993).
18. Grignani, F. *et al*. Effects on differentiation by the promyelocytic leukemia PML/RARalpha protein depend on the fusion of the PML protein dimerization and RARalpha DNA binding domains. *EMBO J.* **15,** 4949–4958 (1996).
19. Horlein, A. J. *et al*. Ligand-independent repression by the thyroid hormone receptor mediated by a nuclear receptor co-repressor. *Nature* **377,** 397–403 (1995).
20. Dhordain, P. *et al*. SMRT binds the BTB/POZ repressing domain of the LAZ3/BCL6 oncoprotein. *Proc. Natl Acad. Sci. USA* **94,** 10727–10767 (1997).
21. Yoshida, M., Kijima, M., Akita, M. & Beppu, T. Potent and specific inhibition of mammalian histone deacetylase both in vivo and in vitro by trichostatin A. *J. Biol. Chem.* **265,** 17174–17179 (1990).
22. Nagy, L. *et al*. Identification and characterization of a versatile retinoid response element in the mouse tissue transglutaminase gene promoter. *J. Biol. Chem.* **271,** 4355–4365 (1996).
23. Benedetti, L. *et al*. Retinoic-induced differentiation of acute promyelocytic leukemia involves PML-RARα-mediated increase of type II transglutaminase. *Blood* **87,** 1939–1950 (1996).
24. Borrow, J. *et al*. The translocation t(8;16)(p11;p13) of acute myeloid leukaemia fuses a putative acetyltransferase to the REB-binding protein. *Nature Genet.* **14,** 33–41 (1996).
25. Zamir, I. *et al*. A nuclear hormone receptor coreceptor mediates transcriptional silencing by receptors with distinct repression domains. *Mol. Cell. Biol.* **16,** 5458–5465 (1996).
26. Nervi, C. *et al*. Characterisation of the PML/RAR chimeric product of the APL-specific t(15;17) translocation. *Cancer Res.* **52,** 3687–3692 (1992).
27. Bartl, S. *et al*. Identification of mouse histone deacetylase I as a growth-factor inducible gene. *Mol. Cell. Biol.* **17,** 5033–5043 (1997).
28. Sundstrom, C. & Nilsson, K. Establishment and characterization of a human histiocytic lymphoma cell line (U-937). *Int. J. Cancer* **17,** 565–577 (1976).
29. Lin, R. J. *et al*. Role of the histone deacetylase complex in acute promyelocytic leukaemia. *Nature* **391,** 811–814 (1998).

Acknowledgements. We thank P. P. DiFiore, K. Ozato, K. Helin, T. Casini and M. Maccarana for discussions, and C. Matteucci, S. DiPietro and S. Lupo for technical help. S.D.M., V.G. and M.F. are recipients of fellowships from A.U.L.L., A.I.R.C. and INT (Milan), respectively.

Correspondence and requests for materials should be addressed to P.G.P. (e-mail: pgpelicci@ieo.cilea.it) and S.M. (sminucci@ieo.cilea.it).

correction

The cerebellar leucine-rich acidic nuclear protein interacts with ataxin-1

Antoni Matilla, Beena T. Koshy, Christopher J. Cummings, Toshiaki Isobe, Harry T. Orr & Huda Y. Zoghbi

Nature **389,** 974–978 (1997)

At the time of submission of this Letter, it escaped our attention that murine and human LANP sequences had previously been reported under different names in the following papers:

1. Vaesen, M. *et al*. Purification and characterization of two putative HLA class II associated proteins: PHAPI and PHAPII. *Biol. Chem. Hoppe-Seyler* **375,** 113–126 (1994).
2. Li, M., Makkinje, A. & Damuni, Z. Molecular identification of I1PP2A, a novel potent heat-stable inhibitor protein of protein phosphatase 2A. *Biochemistry* **35,** 6998–7002 (1996).
3. Chen, T.-H. *et al*. Structure of pp32, an acidic nuclear protein which inhibits oncogene-induced formation of transformed foci. *Mol. Biol. Cell.* **7,** 2045–2056 (1996).
4. Ulitzur, N., Humbert, M. & Pfeffer, S. R. Mapmodulin: A possible modulator of the interaction of microtubule-associated proteins with microtubules. *Proc. Natl Acad. Sci. USA* **94,** 5084–5089 (1997).

Although the gene products reported in these papers were isolated from peripheral tissues, the levels of LANP in cerebellar RNA are significantly higher than in peripheral tissues. Hence the central conclusion of our paper is unchanged. □

erratum

Fear conditioning induces associative long-term potentiation in the amygdala

Michael T. Rogan, Ursula V. Stäubli & Joseph E. LeDoux

Nature **390,** 604–607 (1997)

In Fig. 1a of this Letter, the labelling for the control rat (bottom panel) was erroneously relettered as 'Unpaired/Paired/Paired', whereas it should have read 'Unpaired/Unpaired/Unpaired'.

Also, the report of raw (not normalized) values of slope and amplitudes before training (third paragraph) should read 'slope: conditioned group, $-1.649 \pm 0.425\,\mu V\,ms^{-1}$, control group, $-2.329 \pm 0.346\,\mu V\,ms^{-1}$; *t*-test, $P > 0.05$; amplitude: conditioned group, $14.186 \pm 4.103\,\mu V$, control group, $18.116 \pm 4.214\,\mu V$; *t*-test, $P > 0.05$)'. Finally, on the third line of page 606, $P < 0.01$ (not >0.01 as published). □

diluted in PBS. Either 1 : 100 dilutions of anti-flag M5 monoclonal antibodies (Kodak), anti-ataxin-1 11750V (1 : 100) or anti-ataxin-1 11750VII (1 : 200) polysera[8] were used as primary antibodies. Anti-SC35 hybridoma supernatant[12] was used undiluted. Anti-PML (1 : 200) polysera[5] and anti-PML monoclonal antibody 5E10 (1 : 10 dilution)[4] were used. The anti-Myc Tag monoclonal antibody 9E10 (from V. Bardwell, University of Minnesota) was used to detect BCL-6. Anti-p80-coilin antibody[25,26] was used to visualize coiled bodies. Goat anti-mouse conjugated to FITC (Caltag), goat anti-rabbit conjugated to lissamine rhodamine (Accurate Chemical and Scientific), goat-anti rabbit and goat anti-mouse conjugated to Cy2, Cy3 or Cy5 (Jackson ImmunoResearch) were used as secondary antibodies. Propidium iodide diluted in PBS (1 $\mu g\,ml^{-1}$) was used to stain nucleic acid. A subset of cells was also stained with bisbenzimide (0.001%) 10 min RT (Hoechst 33258 Sigma) as a transfection control. Images were collected and processed as described above.

Preparation of nuclear matrix. COS-1 cells seeded on coverslips were used for nuclear matrix preparations 48 h after transfection, as described previously[15]. Isolated matrices on coverslips were stained by immunofluorescence as described above. Nuclear matrix preparations from transgenic mice cerebella and COS-7 cells were carried out as described[27–29]. Immunoblotting was performed as described[8]. Nuclei were extracted with SK buffer (10 mM PIPES, pH 6.8, 300 mM sucrose, 100 mM NaCl, 3 mM $MgCl_2$, 1 mM EGTA, 0.5% Triton X-100, 1.2 mM PMSF, 2 mM vanadyladenosine and protease inhibitors) for 3 min at 4 °C. Pelleted nuclei were suspended in digestion buffer (SCK plus 50 mM NaCl) with 400 U ml^{-1} of RNase-free DNase I and digested for 50 min at 32 °C. Digested DNA was extracted with 0.25 M $(NH_4)_2SO_4$ and washed with 2 M NaCl in digestion buffer. For COS-7 cells, 2×10^6 cells were extracted analogous to nuclear matrix preparation from transgenic mice, except that extractions were carried out on whole cells instead of isolated nuclei.

Received 9 July; accepted 8 September 1997.

1. Zoghbi, H. Y. & Orr, H. T. Spinocerebellar ataxia type 1. *Semin. Cell Biol.* **6,** 29–35 (1995).
2. Ross, C. A. When more is less: Pathogenesis of glutamine repeat neurodegenerative diseases. *Neuron* **15,** 493–496 (1995).
3. Burright, E. N. *et al.* SCA1 transgenic mice: a model for neurodegeneration caused by an expanded CAG trinucleotide repeat. *Cell* **82,** 937–948 (1995).
4. Stuurman, N. *et al.* A monoclonal antibody recognizing nuclear matrix-associated nuclear bodies. *J. Cell Sci.* **101,** 773–784 (1992).
5. Weis, K. *et al.* Retinoic acid regulates aberrant nuclear localization of PML-RAR alpha in acute promyelocytic leukemia cells. *Cell* **76,** 345–356 (1994).
6. Koken, M. H. *et al.* The t(15;17) translocation alters a nuclear body in a retinoic acid-reversible fashion. *EMBO J.* **13,** 1073–1083 (1994).
7. Dyck, J. A. *et al.* A novel macromolecular structure is a target of the promyelocyte-retinoic acid receptor oncoprotein. *Cell* **76,** 333–343 (1994).
8. Servadio, A. *et al.* Expression analysis of the ataxin-1 protein in tissues from normal and spinocerebellar ataxia type 1 individuals. *Nature Genet.* **10,** 94–98 (1995).
9. Matilla, A. *et al.* Ataxin-1, the SCA1 gene product, is required for learning tasks mediated by both the hippocampus and cerebellum. *Proc. Natl Acad. Sci. USA* (submitted).
10. Robitaille, Y., Schut, L. & Kish, S. J. Structural and immunocytochemical features of olivopontocerebellar atrophy caused by the spinocerebellar ataxia type 1 (SCA-1) mutation define a unique phenotype. *Acta Neropathol.* **90,** 572–581 (1995).
11. Spector, D. L. Macromolecular domains within the cell nucleus. *Annu Rev. Cell Biol.* **9,** 265–315 (1993).
12. Fu, X. D. & Maniatis, T. Factor required for mammalian spliceosome assembly is localized to discrete regions in the nucleus. *Nature* **343,** 437–441 (1990).
13. Raska, I. *et al.* Immunological and ultrastructural studies of the nuclear coiled body with autoimmune antibodies. *Exp. Cell Res.* **195,** 27–37 (1991).
14. Dhordain, P. *et al.* The BTB/POZ domain targets the LAZ3/BCL6 oncoprotein to nuclear dots and mediates homomerisation in vivo. *Oncogene* **11,** 2689–2697 (1995).
15. Bisotto, S., Lauriault, P., Duval, M. & Vincent, M. Colocalization of a high molecular mass phosphoprotein of the nuclear matrix (p255) with spliceosomes. *J. Cell Sci.* **108,** 1873–1882 (1995).
16. Roizin, S. S. & Liu, J. C. Neuronal nuclear-cytoplasmic changes in Huntington's Chorea: electron microscope investigations. *Adv. Neurol.* **23,** 95–122 (1979).
17. Tellez-Nagel, I., Johnson, A. B. & Terry, R. D. Studies on brain biopsies of patients with Huntington's chorea. *J. Neuropathol. Exp. Neurol.* **33,** 308–332 (1974).
18. Roos, R. A. C. & Bots, G. T. A. M. Nuclear membrane indentations in Huntington's Chorea. *J. Neurol. Sci.* **61,** 37–47 (1983).
19. Paulson, H. L. *et al.* Intranuclear inclusions of expanded polyglutamine protein in spinocerebellar ataxia type 3. *Neuron* **19,** 333–344 (1997).
20. Davies, S. W. *et al.* Formation of neuronal intranuclear inclusions (NII) underlies the neurological dysfunction in mice transgenic for the HD mutation. *Cell* **90,** 537–548 (1997).
21. Matilla, A. *et al.* The cerebellar leucine-rich acidic nuclear protein interacts with ataxin-1. *Nature* **389,** 974–978 (1997).
22. Cattoretti, G. *et al.* Antigen unmasking on formalin-fixed, paraffin-embedded tissue sections. *J. Pathol.* **171,** 83–98 (1993).
23. Banfi, S. *et al.* Identification and characterization of the gene causing type 1 spinocerebellar ataxia. *Nature Genet* **7,** 513–520 (1994).
24. Ausubel, F. M. *et al.* in *Current Protocols in Molecular Biology* 9.2.1–9.2.3 (John Wiley, New York, 1996).
25. Andrade, L. E., Tan, E. M. & Chan, E. K. Immunocytochemical analysis of the coiled body in the cell cycle and during cell proliferation. *Proc. Natl Acad. Sci. USA* **90,** 1947–1951 (1993).
26. Chan, E. K., Takano, S., Andrade, L. E., Hamel, J. C. & Matera, A. G. Structure, expression and chromosomal localization of human p80-coilin gene. *Nucleic Acids Res.* **22,** 4462–4469 (1994).
27. Tawfic, S. & Ahmed, K. Association of casein kinase 2 with nuclear matrix. Possible role in nuclear matrix protein phosphorylation. *J. Biol. Chem.* **69,** 7489–7493 (1994).
28. Fey, E. G. & Penman, S. Nuclear matrix proteins reflect cell type origin in cultured human cells. *Proc. Natl Acad. Sci. USA* **85,** 121–125 (1988).
29. Berezney, R. & Coffey, D. S. Nuclear matrix isolation and characterization of a framework structure from rat liver nuclei. *J. Cell Biol.* **73,** 616–632 (1977).

Acknowledgements. We thank V. Bardwell for assistance with the BCL-6 transfections; E. N. Burright for assistance with SCA1 transgenic mice; D. Saxon for assistance with tissue sectioning and staining; G. Sedgewick for assistance with confocal microscopy and image processing; D. Armstrong for assistance in analysis of SCA1 human tissue; T. Maniatis for the anti-SC35 antibody; A. Dejean for the anti-PML polysera; R. Van Driel for the anti-PML monoclonal antibody 5E10; and E. K. Chan for the anti-p80-coilin polysera. This work was supported by grants from the National Institute of Neurological Disorders and Stroke of the NIH to H.T.O. and H.Y.Z. H.Y.Z. is a Howard Hughes Medical Institute investigator.

Correspondence and requests for materials should be addressed to H.T.O. (e-mail: harry@lenti.med.umn.edu).

The cerebellar leucine-rich acidic nuclear protein interacts with ataxin-1

Antoni Matilla*, Beena T. Koshy*, Christopher J. Cummings*†, Toshiaki Isobe‡, Harry T. Orr§ & Huda Y. Zoghbi*†‖

*Departments of * Pediatrics, † Molecular and Human Genetics, and Program in Cell and Molecular Biology, Baylor College of Medicine, and ‖ Howard Hughes Medical Institute, Houston, Texas 77030, USA*

‡ Department of Chemistry, Faculty of Science, Tokyo Metropolitan University, Tokyo, Japan

§ Departments of Laboratory Medicine and Pathology, and Biochemistry, and Institute of Human Genetics, University of Minnesota, Minneapolis, Minnesota 55455, USA

Spinocerebellar ataxia type 1 (SCA1) is an autosomal dominant neurodegenerative disorder characterized by ataxia, progressive motor deterioration, and loss of cerebellar Purkinje cells[1]. SCA1 belongs to a growing group of neurodegenerative disorders caused by expansion of CAG repeats, which encode glutamine[2]. Although the proteins containing these repeats are widely expressed, the neurodegeneration in SCA1 and other polyglutamine diseases selectively involves a few neuronal subtypes. The mechanism(s) underlying this neuronal specificity is unknown. Here we show that the cerebellar leucine-rich acidic nuclear protein (LANP)[3] interacts with ataxin-1, the *SCA1* gene product. LANP is expressed predominantly in Purkinje cells, the primary site of pathology in SCA1. The interaction between LANP and ataxin-1 is significantly stronger when the number of glutamines is increased. Immunofluorescence studies demonstrate that both LANP and ataxin-1 colocalize in nuclear matrix-associated subnuclear structures. The features of the interaction between ataxin-1 and LANP, their spatial and temporal patterns of expression, and the colocalization studies indicate that cerebellar LANP is involved in the pathogenesis of SCA1.

The protein ataxin-1, the *SCA1* gene product, is found predominantly in the nucleus in neurons and the cytoplasm in peripheral tissues[4]. In SCA1, there is selective degeneration of cerebellar Purkinje cells and brainstem neurons[1] despite the wide expression pattern of ataxin-1. Cell-specific proteins may mediate the pathogenesis of SCA1 and the other polyglutamine neurodegenerative diseases.

To identify proteins that interact with ataxin-1, we performed a yeast two-hybrid genetic screen[5] using a mutant human ataxin-1 containing 82 glutamines. Yeast expressing mutant ataxin-1 was transformed with a mouse brain cDNA library, and screening of approximately 1×10^7 tryptophan and leucine auxotrophic transformants resulted in the identification of four positive clones. Sequence analysis of these clones identified partial cDNAs encoding 147 amino acids homologous to the rat leucine-rich acidic nuclear

protein (rLANP; expressed in cerebellum and brainstem)[3], ankyrin G (expressed at the nodes of Ranvier and axonal initial segments in brain, spinal cord and peripheral nerve)[6], myo-inositol 1-phosphate synthase (expressed in brain vasculature and peripheral tissues)[7], and the neurotransmitter transporter rB21a (expressed in leptomeninges)[8]. Because LANP was the only protein known to be expressed in tissues affected in SCA1, it was used for additional studies.

The specificity of the interaction between LANP and ataxin-1 was demonstrated by mating yeast containing LANP with a battery of yeast clones of the opposite mating type expressing 10 different proteins. Only yeast containing both LANP and ataxin-1 with either 30 glutamines or 82 glutamines activated both the *lacZ* and *HIS3* reporter genes.

A full-length mouse cDNA clone (*Lanp*) was isolated from a murine cerebellar cDNA library. Alignment of the deduced mouse LANP amino-acid sequence with those from rat and bovine LANP sequences revealed 98.4% and 92.7% amino-acid identity, respectively. To test the reproducibility of the interaction between LANP and ataxin-1, the full-length mouse *Lanp* cDNA was subcloned into the pAS2-CYH2 vector and the 82-glutamine ataxin-1[82] into the pACT2 vector. When these two clones were co-transformed into yeast, histidine prototrophy and strong β-galactosidase activity were detected.

To define the regions of ataxin-1 that interact with LANP, bait constructs containing different regions of the *SCA1* cDNA were generated[9] and transformed into yeast expressing *Lanp* cDNA. Activation of the *lacZ* reporter gene was noted when ataxin-1 subclones spanning the glutamine repeats, or the last 268 amino acids, were used (Fig. 1). However, the strongest interaction between the two proteins was obtained when full-length ataxin-1 containing 82 glutamines was used. In contrast, no interaction was detected when the first 195 amino acids or amino acids 277–579 of ataxin-1 were used as bait. These results demonstrate that LANP interacts with ataxin-1, and that the interaction is modulated by the number of glutamines. The fact that LANP also interacts with ataxin-1 outside the polyglutamine domain suggests that the interaction between LANP and ataxin-1 is relevant for the cellular function of both proteins. The portion of LANP interacting with ataxin-1 is the first 147 amino acids, containing five leucine-rich repeats (LRRs), an amphipathic motif known to mediate protein–protein interactions[10].

To determine whether the strength of the interaction between ataxin-1 and LANP was influenced by the number of glutamines, we assayed β-gal activity using two different approaches. First, we assayed the sensitivity of the interaction using filter lifts of yeast grown on plates. Yeast containing ataxin-1[82]/LANP turned blue in a shorter time (15 min) than yeast containing ataxin-1[30]/LANP (~4 h), or mouse ataxin-1[2]/LANP (~7 h) (Fig. 2a). Second, β-gal activity was quantified in liquid cultures of yeast containing LANP and ataxin-1 with either 2, 30 or 82 glutamines. The interaction of ataxin-1 and LANP was significantly increased (~10-fold) with 82 glutamines compared with 30 or 2 glutamines ($F_{2,10} = 302.45$, $P < 0.0001$; Fig. 2b). These results demonstrate that the mutant form of ataxin-1 associates more strongly with LANP.

In situ hybridization studies revealed that rat *Lanp* mRNA is enriched in cerebellar Purkinje cells and granule neurons[3]. The highest expression levels in Purkinje cells are on postnatal day 14 (P14), after which the expression decreases to adult levels. Because the first three postnatal weeks are important for neuronal differ-

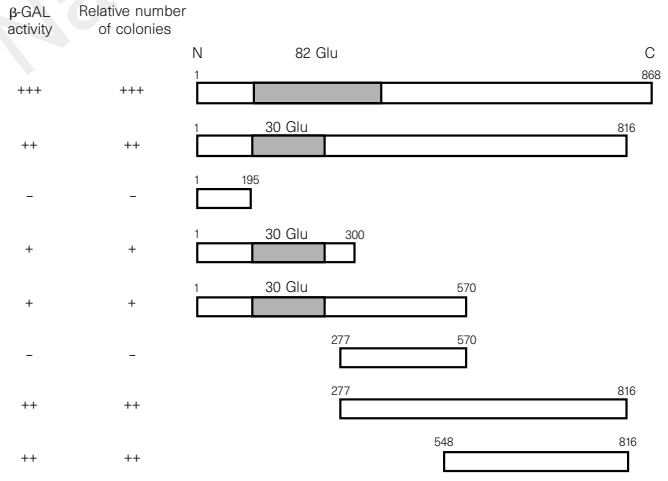

Figure 1 Schematic representation of constructs used in the yeast two-hybrid screen to assay interactions between ataxin-1 and LANP. Numbers indicate the positions of amino acids in ataxin-1. The polyglutamine tract and the C-terminal region (amino acids 570–816) of ataxin-1 interact with LANP. More colonies and a higher level of β-galactosidase activity, as detected by intensity of blue colour, are observed with the full-length mutant ataxin-1[82].

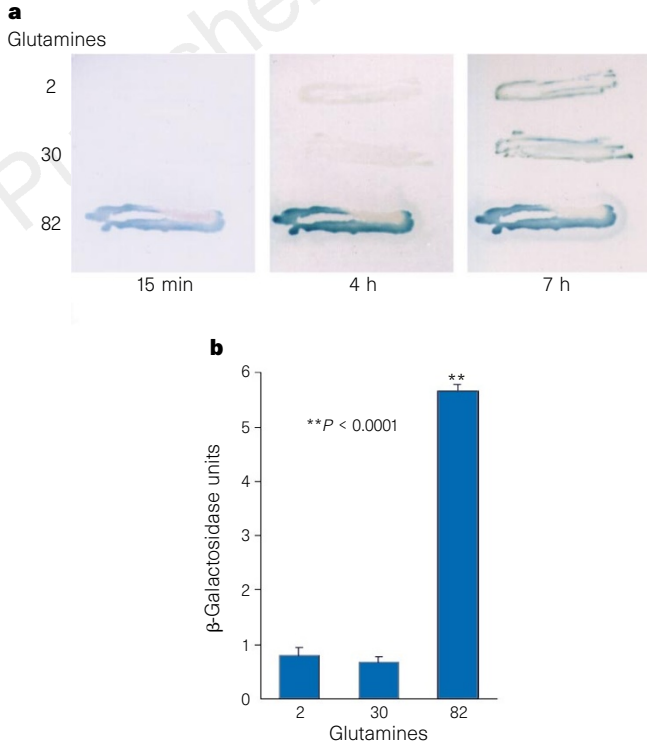

Figure 2 β-Galactosidase assays of the interaction between ataxin-1 and LANP. **a**, Filter-lift assay of β-galactosidase activity in yeast containing LANP and ataxin-1 with either 2, 30 or 82 glutamines. **b**, Liquid assays showing the β-galactosidase activity based on the interaction between LANP and ataxin-1, with either 2, 30, or 82 glutamines in ataxin-1. A significant increase in interaction between ataxin-1 and LANP is noted in the presence of 82 glutamines ($P < 0.0001$). Error bars indicate s.e.m.

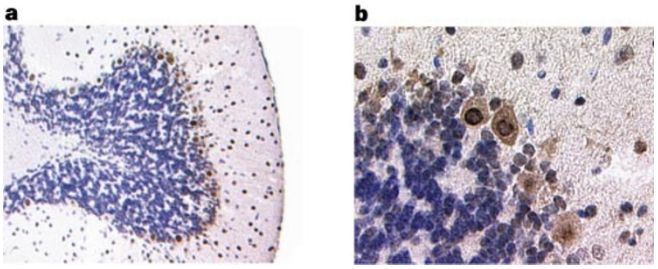

Figure 3 Immunohistochemical staining of LANP in mouse cerebellar cortex. LANP is localized predominantly to the nuclei of Purkinje cells. **a**, Magnification ×275; **b**, ×880.

entiation and synaptogenesis in the rat cerebellum, the temporal expression profile of LANP suggests that this nuclear protein may be involved in cerebellar morphogenesis. We observed a similar temporal expression profile for the *Sca1* gene product. In Purkinje cells, *Sca1* mRNA levels are highest at P14, after which they gradually decrease to adult level[11]. Immunohistochemical analysis using anti-LANP antisera in murine brain slices showed the highest levels of LANP in the nuclei of cerebellar Purkinje cells, with much weaker signal in the cytoplasm of Purkinje cells and nuclei of granule cells (Fig. 3). Similarly, ataxin-1 is predominantly nuclear in Purkinje cells, with very low but detectable levels found in the cytoplasm[4]. LANP immunoreactivity was detected, although at lower levels, in the cerebellar deep nuclei, brainstem and thalamus. The expression pattern of LANP in Purkinje cells and the overlapping spatial and temporal expression patterns of both LANP and ataxin-1 make LANP an excellent candidate to be a cell-specific target implicated in SCA1 pathology. Recently, we have identified the human LANP homologue confirming the existence of this protein in humans. The

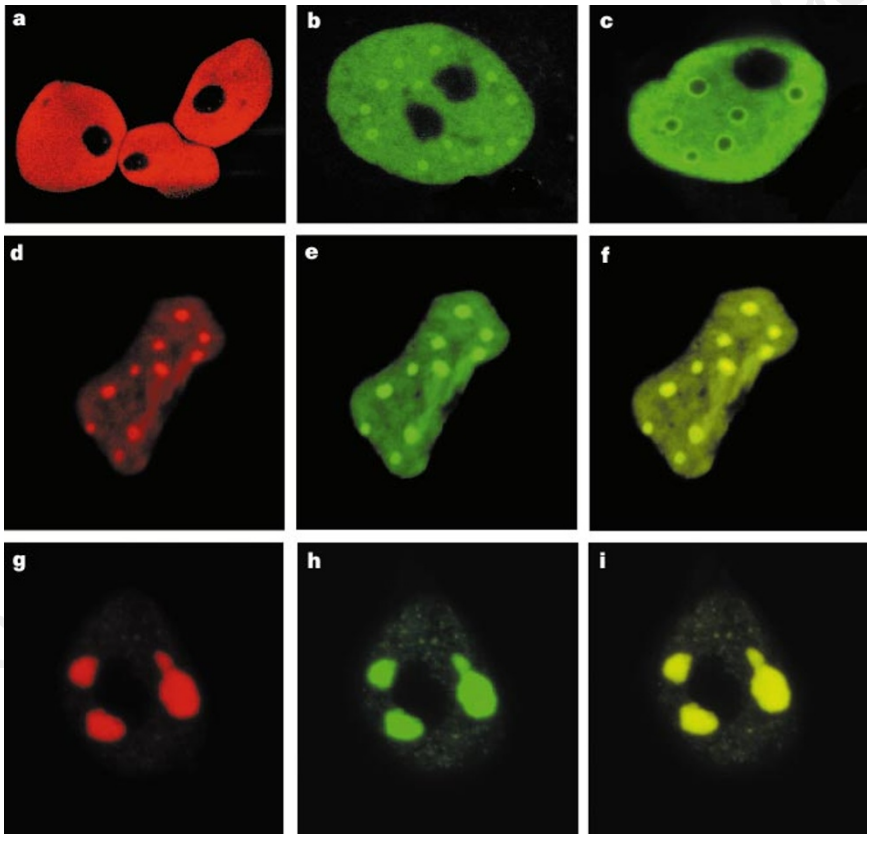

Figure 4 Colocalization of LANP and ataxin-1 in subnuclear structures by confocal immunofluorescence in COS-7 cells. Anti-Flag antibody (red) and ataxin-1 antisera (green) were used to detect LANP and ataxin-1, respectively. **a**, The distribution of LANP when expressed alone in COS-7 cells is homogeneous in the nucleus. Ataxin-1 with either 30 glutamines (**b**) or 82 glutamines (**c**) shows both a diffuse nuclear staining pattern as well as discrete subnuclear structures in transiently transfected COS-7 cells. COS-7 cells stably expressing ataxin-1 with either 30 (**d**–**f**), or 92 (**g**–**i**) glutamines were transiently transfected with LANP. The size of the structures is largest in the cells expressing ataxin-1 with either 82 (**c**) or 92 (**h**) glutamines. **d**, **g**, Immunofluorescence demonstrates that, in presence of ataxin-1, LANP localizes to the subnuclear structures. **f**, **i** Overlays demonstrating the colocalization of ataxin-1 and LANP. Magnification, ×3,500.

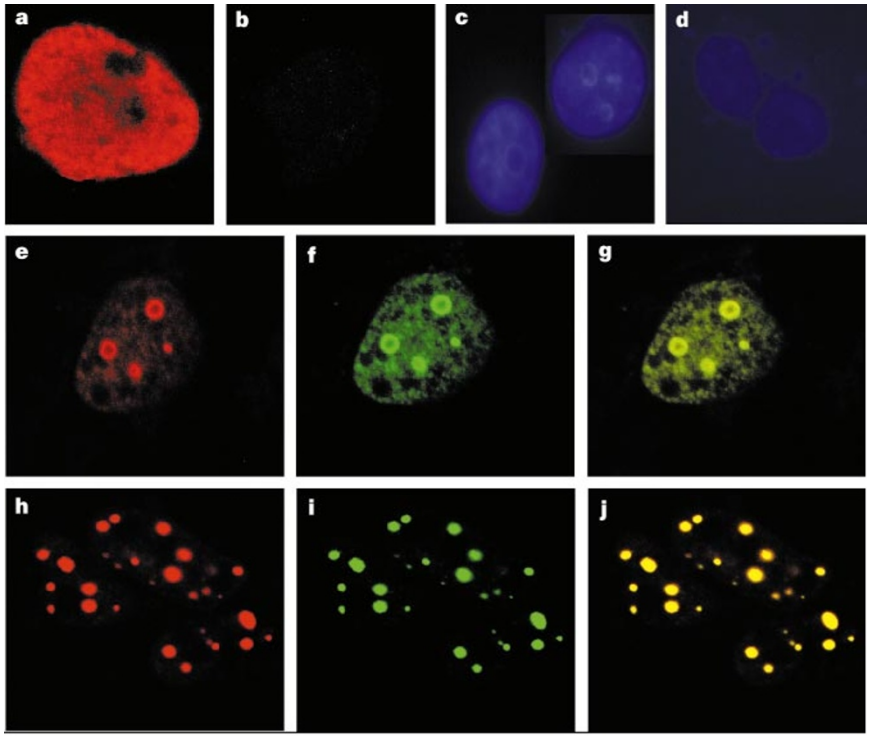

Figure 5 Confocal microscopy of isolated nuclear matrix from COS-7 cells demonstrates localization of LANP to the nuclear matrix in the presence of ataxin-1. Anti-Flag antibody (red) and ataxin-1 antisera (green) were used to detect LANP and ataxin-1, respectively. **a**, Nuclei in unextracted COS-7 cells expressing LANP alone show a homogeneous staining pattern. **b**, Nuclear matrix preparations from LANP-transfected cells show absence of LANP staining. **c**, **d**, DAPI staining before (**c**) and after (**d**) DNaseI treatment demonstrates the removal of nucleic acids in the nuclear matrix preparation (**d**). **e**–**j**, Nuclear matrix preparations from COS-7 cells cotransfected with LANP and ataxin-1 containing either 30 (**e**–**g**) or 82 (**h**–**j**) glutamines demonstrate that LANP localizes to the nuclear matrix through its interaction with ataxin-1 (**g**, **j**). Magnification ×3,500.

mouse and human proteins have 89% amino-acid identity (GenBank accession numbers AF022957 and AF025684, respectively).

Ataxin-1 localizes to subnuclear structures in COS-1 cells and cerebellar Purkinje cells of SCA1 patients and transgenic mice[12]. The number and the size of these structures depend on the number of glutamines, and ataxin-1 is present in the nuclear matrix fraction[12]. We analysed the localization pattern of LANP in COS-7 cells that were either transiently expressing ataxin-1 with 30 or 82 glutamines, or stably expressing ataxin-1 with 30 or 92 glutamines. When LANP was transfected alone into COS-7 cells, a homogeneous staining pattern was noted in the nucleus (Fig. 4a). In contrast, COS-7 cells expressing either LANP and ataxin-1[30] (Fig. 4d–f) or LANP and expanded ataxin-1[82] or ataxin-1[92] (Fig. 4g–i) demonstrated an altered staining pattern of LANP, with LANP colocalizing with ataxin-1 in the subnuclear structures (Fig. 4f, i). These results demonstrate that LANP, which by itself does not form nuclear aggregates, is recruited to the subnuclear structures through its interaction with ataxin-1. To demonstrate the specificity of the interaction between ataxin-1 and LANP in cultured cells, we overexpressed ataxin-1 and the nuclear transcription factor SP1 in COS-7 cells and demonstrated that SP1 does not colocalize with ataxin-1 in the subnuclear structures (data not shown). Finally, we analysed the localization of LANP using an *in situ* nuclear matrix preparation[13], and observed that when LANP was expressed alone it was removed efficiently from the nucleus after detergent extraction (Fig. 5a, b). In contrast, when LANP was coexpressed with ataxin-1 in COS-7 cells it localized to the salt-resistant subnuclear structures associated with the nuclear matrix (Fig. 5e–j). These results demonstrate that LANP is sequestered and localized to the nuclear matrix through its interaction with ataxin-1. Co-immunoprecipitation experiments failed to demonstrate an interaction between ataxin-1 and LANP. Biochemical isolation of LANP and ataxin-1 using an *in vitro* nuclear matrix extraction protocol[13,14] demonstrated that LANP was easily removed by detergent treatment (data not shown). These data, together with the *in situ* immunolocalization data, lead us to believe that the structural integrity of the nucleus is essential for the interaction between ataxin-1 and LANP.

The data available to date strongly support a gain-of-function model of pathogenesis for SCA1. Transgenic mice overexpressing a mutant form of a human *SCA1* cDNA in Purkinje cells develop ataxia and Purkinje-cell degeneration[15]. In contrast, mice lacking the *Sca1* gene have learning and memory deficits without evidence of ataxia[16]. The specificity of the neuronal phenotype is probably determined both by the expression levels of ataxin-1 and by interactions with neuronal specific nuclear targets. The temporal and cell-specific expression pattern of LANP in cerebellar Purkinje cells, as well as its enhanced interaction with mutant ataxin-1, renders LANP an excellent candidate to be a cell-specific target in SCA1 pathogenesis. The fact that mutant ataxin-1 leads to subnuclear alterations in SCA1 patients, SCA1 transgenic mice, and COS-1 cells[12] suggests that the pathogenesis of SCA1 is mediated through the disturbance of normal nuclear function.

LANP belongs to a group of proteins that contain LRRs. Proteins containing LRRs occur in a wide range of organisms, and several are known to be involved in early morphogenesis and cell adhesion[17]. Although very few properties are shared amongst LRR-containing proteins, most are involved in protein–protein interactions, and about half are involved in known signal-transduction pathways[10,17]. The localization of LANP to the large subnuclear structures formed by mutant ataxin-1 may keep LANP from exerting its normal function, lead to the sequestration of additional nuclear factors, or promote its interaction with incorrect nuclear targets. Although the precise function of LANP is not yet known, its temporal expression pattern during cerebellar development suggests that it may be involved in cerebellar morphogenesis. Generation of mice with a null mutation for LANP or overexpressing LANP in Purkinje cells should provide further insight into the role of LANP in SCA1 pathology. □

Methods

Plasmids and yeast strains. A human *SCA1* cDNA containing 82 CAG repeats was subcloned in the pAS2-CYH2 vector, which contains the GAL4 DNA-binding domain[18], and transformed into the yeast strain Hf7c[19]. A Hf7c yeast clone expressing ataxin-1[82] was transformed with a mouse brain library cloned in the pACT2 vector containing the GAL4 activation domain[20]. Yeast clones growing in SC-His/-Trp/-Leu were tested for β-gal activity using the filter-lift method[21]. To assess the specificity of the interaction between ataxin-1[82] and LANP, Y187 yeast, containing the first 147 amino acids of LANP was mated with Hf7c containing ataxin-1[30], ataxin-1[82], Lamin, SNF1, Tat, Cdc25, p53, Rb, Rev, cyclin D1, Cdk2 and Cdk6, to form diploids. Diploids were tested for β-gal activity. The bait constructs containing ataxin-1 with 30 glutamines and different regions of the *SCA1* cDNA were as previously described[9]. A partial murine *Sca1* cDNA (amino acids 1–226) containing two CAG repeats was cloned into the pAS2-CYH2 vector.

Liquid assay of β-galactosidase activity. A liquid assay of four independent Y190 transformants containing LANP and ataxin-1 with either 2, 30 or 82 glutamines, each assay performed in triplicate, was performed as described[22]. The values (mean ± s.d.) were averaged and ANOVA was performed to evaluate the statistical significance.

Immunohistochemistry and immunofluorescence. Immunohistochemical staining was performed using a bovine anti-LANP polyclonal antibody[3] on mouse brain sections[4]. Transient expression of ataxin-1 and LANP in COS-7 cells was done according published protocols[15]. Full-length mouse *Lanp* was subcloned in the pFlag–CMV-2 vector (Kodak). COS-7 cells stably expressing human ataxin-1 with either 2, 30 or 92 glutamines were generated using the pcDNA3.1/HIS-C expression vector system (Invitrogen). Cells were transfected and passaged at least three times in the presence of 250 μg ml^{-1} G418 in DMEM (Gibco/BRL). Cells were fixed for 10 min in 3.7% formaldehyde in phosphate-buffered saline (PBS) 48 h after transfection, permeabilized in acetone at −20 °C, and incubated for 60 min at 37 °C in a humid chamber with rabbit polyclonal antibodies (1 : 100) recognizing ataxin-1 (11750V)[4] and/or mouse monoclonal antibodies (1 : 100) M2 (Kodak) recognizing the Flag epitope. Subsequently, cells were incubated with either anti-rabbit-FITC or anti-mouse-TRITC (1 : 100, Vector Laboratories), mounted in antifade solution (Vectashield mounting medium, Vector Laboratories), and analysed by laser confocal microscopy (BioRad 1024).

Cytoskeletal and nuclear matrix preparation. Cytoskeletal and nuclear matrix preparations were carried out 48 h after transfection as described[13]. Briefly, coverslips were rinsed with PBS, extracted on ice with cytoskeletal buffer contain (in mM) 10 PIPES, pH 6.8, 300 sucrose, 100 NaCl, 3 $MgCl_2$, 1 EGTA, 0.5% Triton X-100, 1.2 PMSF, 2 vanadylribonucleoside complex and 1 × protease inhibitors (Complete, Boehringer). For cytoskeletal preparations, cells were fixed with 3.7% formaldehyde for 20 min on ice and rinsed twice with PBS before immunodetection. For the nuclear matrix preparations, cytoskeletal coverslips were digested with 400 U ml^{-1} of RNase-free DNaseI (Boehringer) in digestion buffer (cytoskeletal buffer with 50 mM NaCl) for 50 min at 32 °C followed by extraction with 0.25 M ammonium sulphate and 2 M NaCl in digestion buffer. Cells were fixed with 3.7% formaldehyde in digestion buffer on ice, rinsed in PBS, and incubated with blocking solution (5% Blotto, BioRad) for 30 min at room temperature. Immunodetection was performed as above. Cells were counterstained in mounting media containing DAPI (1 μg ml^{-1}), and analysed by laser confocal microscopy (BioRad 1024).

Received 9 July; accepted 8 September 1997.

1. Zoghbi, H. & Orr, H. Spinocerebellar ataxia type 1. *Semin. Cell Biol.* **6,** 29–35 (1995).
2. Orr, H. *et al.* Expansion of an unstable trinucleotide (CAG) repeat in spinocerebellar ataxia type 1. *Nature Genet.* **4,** 221–226 (1993).
3. Matsuoka, K. *et al.* A nuclear factor containing the leucine-rich repeats expressed in murine cerebellar neurons. *Proc. Natl Acad. Sci. USA* **91,** 9670–9674 (1994).
4. Servadio, A. *et al.* Expression analysis of the ataxin-1 protein in tissues from normal and spinocerebellar ataxia type 1 individuals. *Nature Genet.* **10,** 94–98 (1995).
5. Fields, S. & Song, O.-K. A novel genetic system to detect protein-protein interactions. *Nature* **340,** 245–246 (1989).
6. Kordeli, E., Lambert, S. & Bennet, V. AnkyrinG. A new ankyrin gene with neural-specific isoforms localized at the axonal initial segment and node of Ranvier. *J. Biol. Chem.* **270,** 2352–2359 (1995).
7. Wong, Y. H., Kalmbach, S. J., Hartman, B. K. & Sherman, W. R. Immunohistochemical staining and enzyme activity measurements show myo-inositol-1-phosphate synthase to be localized in the

vasculature of brain. *J. Neurochem.* **48,** 1434–1442 (1987).
8. Smith, K. E. *et al.* Molecular cloning of an orphan transporter. A new member of the neurotransmitter transporter family. *FEBS Lett.* **357,** 86–92 (1995).
9. Koshy, B. *et al.* Spinocerebellar ataxia type-1 and spinobulbar muscular atrophy gene products interact with glyceraldehyde-3-phosphate dehydrogenase. *Hum. Mol. Genet.* **5,** 1311–1318 (1996).
10. Kobe, B. & Deisenhofer, J. The leucine-rich repeat: a versatile binding motif. *Trends Biochem. Sci.* **19,** 415–421 (1994).
11. Banfi, S. *et al.* Cloning and developmental expression analysis of the murine homolog of the spinocerebellar ataxia type 1 gene (*Sca1*). *Hum. Mol. Genet.* **5,** 33–40 (1996).
12. Skinner, P. *et al.* Ataxin-1 with an expanded glutamine tract alters nuclear matrix-associated structures. *Nature* **389,** 971–974 (1997).
13. Fey, E. G. & Penman, S. Nuclear matrix proteins reflect cell type of origin in cultured human cells. *Proc.l Natl Acad. Sci. USA* **85,** 121–125 (1988).
14. Berezney, R. & Coffey, D. S. Nuclear matrix isolation and characterization of a framework structure from rat liver nuclei. *J. Cell Biol.* **73,** 616–632 (1977).
15. Burright, E. *et al.* SCA1 transgenic mice: a model for neurodegeneration caused by an expanded CAG trinucleotide repeat. *Cell* **82,** 937–948 (1995).
16. Matilla, A. *et al.* Ataxin-1, the *SCA1* gene product, is required for learning tasks mediated by both the hippocampus and cerebellum. *Proc. Natl Acad. Sci. USA* (submitted).
17. Kobe, B. & Deisenhofer, J. Proteins with leucine-rich repeats. *Curr. Opin. Struct. Biol.* **5,** 409–416 (1995).
18. Harper, J. W., Adami, G. R., Wei, N., Keyomarsi, K. & Elledge, S. J. The p21 Cdk-interacting protein Cip1 is a potent inhibitor of G1 cyclin-dependent kinases. *Cell* **75,** 805–816 (1993).
19. Feilotter, H. E., Hannon, G. J., Ruddell, C. J. & Beach, D. Consctruction of an improved host strain for two hybrid screening. *Nucleic Acids Res.* **22,** 1502–1503 (1994).
20. Durfee, T. *et al.* The retinoblastoma protein associates with the protein phosphatase type 1 catalytic subunit. *Genes Dev.* **7,** 555–569 (1993).
21. Breeden, L. & Nasmyth, K. Regulation of the yeast HO gene. *Cold Spring Harb. Symp. Quant. Biol.* **50,** 643–650 (1985).
22. Rose, M. & Botstein, D. Construction and use of gene fusions to lacZ (β-galactosidase) that are expressed in yeast. *Methods Enzymol.* **101,** 167–180 (1983).

Acknowledgements. We thank S. Elledge for the Y187 and Y190 yeast strains, pAS2-CYH2 and pACT2 vectors, and constructs expressing Lamin, SNF1, Tat, Cdc25, p53, Rb, Rev, cyclin D1, Cdk2 and Cdk6; E. N. Olson for the mouse brain cDNA library; D. Beach for the Hf7c yeast strain; D. Armstrong for neuropathological expertise; S. Y. Tsai for the expression vector containing SP1; R. C. Atkinson for assistance with confocal microscopy; R. Phillips and B. Antalffy for technical expertise; and A. Beaudet for critically reading the manuscript. This work was supported by grants from the NIH to H.Y.Z. and H.T.O. and by the Baylor College of Medicne Mental Retardation Research Center. A.M. was supported by a postdoctoral fellowship from the Spanish Ministerio de Educación y Ciencia.

Correspndence and requests for materials should be addressed to H.Y.Z. (e-mail: hzoghbi@bcm.tmc.edu).

Cutaneous lymphocyte antigen is a specialized form of PSGL-1 expressed on skin-homing T cells

Robert C. Fuhlbrigge*, J. David Kieffer*, Dieter Armerding* & Thomas S. Kupper

Harvard Skin Disease Research Center, Division of Dermatology, Department of Medicine, Brigham and Women's Hospital, 75 Francis Street, Boston, Massachusetts 02115, USA
* *These authors contributed equally to this work.*

T cells play a pathogenic role in many inflammatory and certain malignant skin diseases, including psoriasis, atopic and allergic contact dermatitis, and cutaneous T-cell lymphoma[1–6]. Memory T cells that infiltrate the skin express a unique skin-homing receptor called cutaneous lymphocyte-associated antigen (CLA), a carbohydrate epitope that facilitates the targeting of T cells to inflamed skin[1,7,8]. CLA is defined by both its reactivity with a unique monoclonal antibody, HECA-452, and its activity as a ligand for E-selectin[2,9–11], but the structure of the protein component of CLA has not previously been defined. Here we report that CLA is an inducible carbohydrate modification of P-selectin glycoprotein ligand-1 (PSGL-1), a known surface glycoprotein that is expressed constitutively on all human peripheral-blood T cells. Cultured peripheral-blood T cells can be differentiated into CLA-bearing cells, which bind both E-selectin and P-selectin, or CLA-negative cells, which bind P-selectin but do not bind E-selectin, suggesting that there is independent regulation of selectin-binding phenotypes. We propose that differential post-translational modification of a single cell-surface receptor, PSGL-1, mediated by fucosyltransferase VII, serves as a mechanism for regulating tissue-specific homing of memory T cells.

The accumulation of memory T cells in non-lymphoid peripheral tissues is typically initiated by the interaction of glycoprotein ligands on the T-cell surface with E-selectin or P-selectin expressed on vascular endothelium[12–15]. Previous studies have shown that distinct subsets of memory T cells tether and roll on E-selectin and P-selectin *in vitro*, suggesting that T-cell binding to E-selectin and P-selectin is mediated by independent cell-surface receptors[2,11,16]. T cells are known to bind P-selectin through PSGL-1, a well-characterized mucin-like glycoprotein that seems to be the sole physiological ligand for P-selectin[17]. To function as an effective P-selectin ligand, the PSGL-1 protein must be modified by appropriate glycosylation and tyrosine sulphation. The E-selectin ligands on T cells, in contrast, are not as well characterized. Although CLA is expressed by a sizeable minority of peripheral-blood T cells, activation and expansion under standard T-cell culture conditions results in loss of expression, complicating the analysis of its structure and function. Methods have been described that partly reverse this inhibition, but these result in only low-level expression[8,18].

We have developed conditions, using a serum-free medium (XVIVO15), that result in the induction and maintenance of high levels of CLA on virtually all peripheral blood T cells (Fig. 1b). These conditions are similar to those reported to induce CLA expression on cultured vaccine-primed lymph-node cells[19]. Parallel activation and culture in conventional T-cell growth media with fetal calf serum (CG/RPMI-FCS) resulted in an initially low stimulation (not shown), followed by loss of CLA expression within 7 days (Fig. 1c). The basis for these properties of serum-free medium is yet to be established, although the addition of FCS to XVIVO15 medium only partly inhibited CLA expression (not shown).

To confirm that CLA expressed on T cells cultured *in vitro* was similar to that on unstimulated peripheral blood T cells, HECA-452-reactive cells were immunomagnetically purified from peripheral-blood mononuclear cells and compared with T cells expanded *in vitro*. The level of CLA expressed on HECA-selected

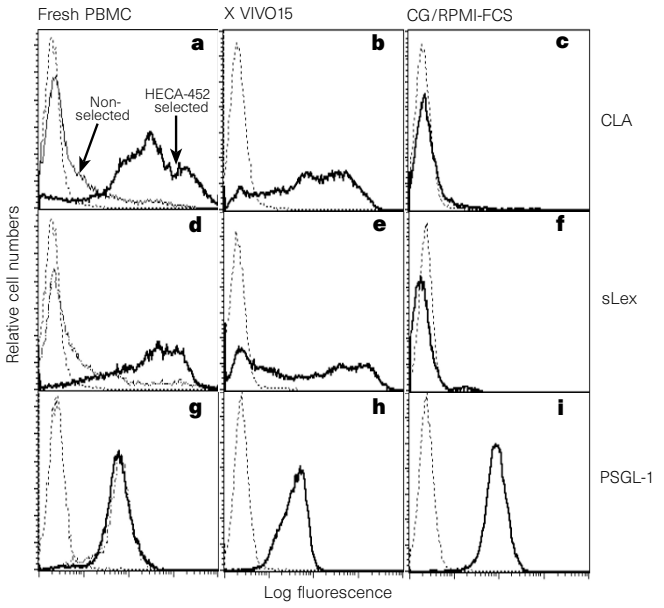

Figure 1 Expression of CLA, sLe^x and PSGL-1 by fresh and cultured PBMCs. Freshly prepared human PBMCs were stained unselected and after selection for HECA-452-expressing cells. HECA-selected cells (thick line) expressed high levels of CLA (HECA-452 mAb) (**a**) and sLe^x (CSLEX-1 mAb) (**d**) relative to unselected cells (thin line). PBMCs cultured in XVIVO15 medium expressed high levels of CLA (**b**) and sLe^x (**e**); PBMCs cultured in CG/RPMI-FCS medium showed minimal staining for either CLA (**c**) or sLe^x (**f**). PSGL-1 was expressed at similar levels in all groups (**g–i**). The broken lines represent staining with isotype-matched control antibodies.

stimuli similar to that used for the psychophysical experiment. Pairs of textures either containing or not containing an embedded contour were generated and processed using the model. The longest blob was calculated for both images, and the image producing the longer of the two was selected as the one containing the contour. Performance of the model was determined as a function of path angle (the orientational difference between successive elements of the contour).

Received 9 May; accepted 9 September 1997.

1. Field, D. J., Hayes, A. & Hess, R. F. Contour integration by the human visual system: evidence for a local "association field". *Vision Res.* **33,** 173–193 (1993).
2. Aubert, H. & Foerster, E. Unter suchungen über raumsinn der retina. *Albrecht v. Graefes Arch. Opthalmol.* **3,** 1–37 (1857).
3. Schneider, G. E. Two visual systems. *Science* **163,** 895–902 (1969).
4. von der Malsburg, C. in *Synergetics of the Brain* (ed. Basar, E., Flohr, H., Haken, H. & Mandall, A. J.) 238–249 (Springer, Berlin, 1983).
5. von der Malsburg, C. & Singer, W. in *Neurobiology of Neocortex* (eds Rakic, P. & Singer, W.) 69–99 (Wiley, Chichester, 1988).
6. Kreiter, A. K. & Singer, W. Global stimulus arrangement determines synchronization of neuronal activity in the awake macaque monkey. *Eur. J. Neurosci.* (suppl.) **7,** 153 (1994).
7. Engel, A. K., Konig, P., Kreiter, A. K., Schillen, T. B. & Singer, W. Temporal coding in the visual cortex: new vistas on integration in the nervous system. *Trends Neurosci.* **15,** 218–226 (1992).
8. Watt, R. J. & Morgan, M. J. A theory of the primitive spatial code in human vision. *Vis. Res.* **25,** 1661–1674 (1985).
9. Wang, Y., Thibos, L. N. & Bradley, A. Undersampling produces non-veridical motion perception, but not necessarily motion reversal, in peripheral vision. *Vision Res.* **36,** 1737–1744 (1996).
10. Gilbert, C. D. & Wiesel, T. N. Columnar specificity of intrinsic horizontal and corticocortical connections in cat visual cortex. *J. Neurosci.* **9,** 2432–2442 (1989).
11. Tso, D. Y. & Gilbert, C. D. The organization of chromatic and spatial interactions in the primate striate cortex. *J. Neurosci.* **8,** 1712–1727 (1988).
12. Phillips, G. & Wilson, H. Orientation bandwidths of spatial mechanisms measured by masking. *J. Opt. Soc. Am.* **62,** 226–232 (1983).
13. Watt, R. J. *Understanding Vision* (Academic, London, 1991).

Acknowledgements. This work was supported by the Canadian MRC (MT 10818).

Correspondence and requests for materials should be addressed to R.F.H. (e-mail: rhess@bradman.vision.mcgill.ca)

Fear conditioning induces associative long-term potentiation in the amygdala

Michael T. Rogan, Ursula V. Stäubli & Joseph E. LeDoux

Center for Neural Science, New York University, 6 Washington Place, New York, New York 10003, USA

Long-term potentiation (LTP) is an experience-dependent form of neural plasticity believed to involve mechanisms that underlie memory formation[1–3]. LTP has been studied most extensively in the hippocampus, but the relation between hippocampal LTP and memory has been difficult to establish[4–6]. Here we explore the relation between LTP and memory in fear conditioning, an amygdala-dependent form of learning in which an innocuous conditioned stimulus (CS) elicits fear responses after being associatively paired with an aversive unconditioned stimulus (US). We have previously shown that LTP induction in pathways that transmit auditory CS information to the lateral nucleus of the amygdala (LA) increases auditory-evoked field potentials in this nucleus[7]. Now we show that fear conditioning alters auditory CS-evoked responses in LA in the same way as LTP induction. The changes parallel the acquisition of CS-elicited fear behaviour, are enduring, and do not occur if the CS and US remain unpaired. LTP-like associative processes thus occur during fear conditioning, and these may underlie the long-term associative plasticity that constitutes memory of the conditioning experience.

To determine whether fear conditioning results in learning-related changes in CS processing that are similar to the effect of LTP induction in auditory CS pathways, we concurrently measured auditory CS-evoked field potentials in LA and CS-evoked fear behaviour, before, during and after fear conditioning in freely behaving rats. The rats were randomly assigned to groups that underwent either fear conditioning (in which the CS and US were paired) or a non-associative control procedure (in which the CS and US were explicitly unpaired). The CS was a 20-s series of acoustic tones (1 kHz, 50 ms, 72 dB) delivered at 1 Hz. The onset of each tone in the series triggered the acquisition of an evoked waveform from the electrode in LA, so that each 20-s CS produced 20 evoked responses. The 100 evoked waveforms from each session (5 CS per session; mean inter-CS interval, 170 s, range 140–200 s) were averaged to yield a mean CS-evoked field potential (CS-EP) for that session. The use of this 'one tone per second' 20-s CS allowed the sampling of CS-evoked activity at 20 points within a single CS, greatly increasing the signal-to-noise ratio of the field potentials under study over that obtainable with the continuous-tone CS typically used in conditioning studies[8–10].

The CS-EPs were quantified by measuring the latency, slope and amplitude of the negative-going potential occurring 15–30 ms after the onset of the tone stimulus, as per our previous study of auditory evoked field potentials in LA[7]. Anatomical and physiological evidence indicates that these field potentials are generated in the LA[6]. A set of CS-EPs for two rats, one from the 'conditioned' group and one from the 'control' group, over the seven sessions of testing and training is shown in Fig. 1a. As previously reported[7], before training the CS elicited a negative-going field potential with a latency of about 18 ms (18.52 ± 3.58 ms across animals). The raw (not normalized) slope and amplitude of these potentials did not differ between the two groups in the baseline tests before training (slope: conditioned group, $-1.649 \pm .425\ \mu V\ ms^{-1}$, control group, $-2.329 \pm .346\ \mu V\ ms^{-1}$; *t*-test, $P > 0.05$, conditioned group, $14.186 \pm 4.103\ \mu V$; control group, 18.116 ± 4.214; *t*-test, $P > 0.05$). As seen in the examples shown (Fig. 1a), paired training led to an increase in the slope and amplitude of the CS-EPs, whereas unpaired training did not. Mean group data of slope and amplitude of CS-EPs, normalized as a percentage of mean baseline measures, are shown in Fig. 1b. For both groups, slope and amplitude were stable for the first two sessions (testing), in which only the CS was presented. Responses in these sessions were used as a baseline from which to measure changes due to training. For the conditioned group, slope and amplitude were unchanged by unpaired presentations of the CS and US in session 3, but increased significantly above baseline in sessions 4 and 5 when the CS was paired with the US (statistics in Fig. 1b). Both measures remained elevated in session 6, in which only the CS was presented, and fell towards baseline in the last session, reflecting the weakening of the CS-US relation by presentations of the CS without the US (extinction trials). The slope and amplitude of the CS-EPs remained statistically unchanged throughout the course of training and testing for the control group (statistics in Fig. 1b). Slope and amplitude did not differ between the groups until pairing occurred, and remained different until the last session (statistics in Fig. 1b). The fact that the two groups received an equal number of CS and US presentations during training, and that unpaired training was not accompanied by increases in CS-EPs in either group, indicates that the effect of paired training on the field potentials in the conditioned group is due to the associative relation of the CS and US and not to nonspecific arousal elicited by either stimulus alone[11].

The differential effects of training on CS-EPs for each member of the control and conditioned groups is shown in Fig. 2. This scattergram demonstrates the consistency with which the control group was unaffected by training and the reliability of the increases in slope and amplitude of the CS-EPs in the conditioned group.

The acquisition of conditioned fear behaviour was evaluated by measuring 'freezing', a characteristic defensive posture expressed in the presence of stimuli that predict danger[12–15]. The amount of time accounted for by freezing was measured during the 20-s CS and also during the 20 s immediately before CS onset (pre-CS period). The latter is a measure of the acquisition of aversive conditioning to the experimental context in which the US is delivered (such as the conditioning chamber); freezing to the experimental context is

independent of the presence or absence of an explicit CS, and is typically seen with both paired and unpaired training[8,10]. In this experiment and pilot studies, the pattern of behaviour exhibited during the 'one tone per second' 20-s CS was in all respects similar to the behaviour exhibited by animals trained with a 20-s continuous tone CS; for example, rats did not respond to the individual tones that made up the CS, but rather behaved as though the 20-s CS period was a continuous tone.

Analyses of variance and post hoc tests of the behavioural data showed the expected result from paired and unpaired training. Thus there was a significant interaction between group and session, owing to the higher level of freezing in the conditioned group in session 6, the first test session after training (statistics in Fig. 1c). This was also the session in which the CS-EP measures differed most between the groups (Fig. 1b). By the next session, freezing responses, like field-potential measures, no longer differed between the groups, showing that the CS–US relation had extinguished. Although both groups froze extensively during training (sessions 3–5), freezing measured in sessions with US presentations is not generally useful as an index of CS-related learning, owing to the confounding effects of the US on freezing behaviour[8].

To further investigate the differential effect of paired versus unpaired training we analysed freezing before the CS and during the CS in the two groups (data not shown). Pre-CS freezing, which reflects conditioning to contextual stimuli[8], did not differ between the conditioned and control groups at any point in the course of

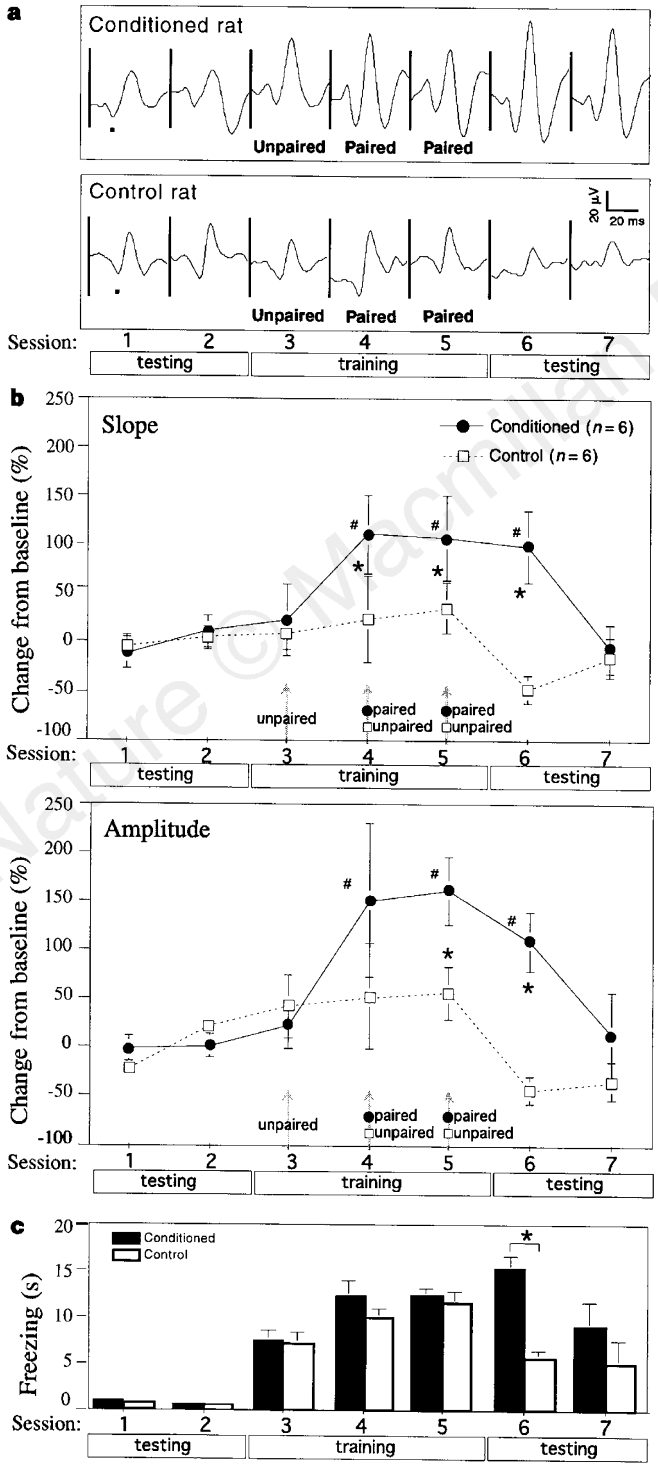

Figure 1 The effect of paired and unpaired training on CS-evoked field potentials and behaviour. Sessions are numbered 1–7; one session occurred per day, except that sessions 3 and 4 occurred on the same day. **a**, CS-evoked field potentials from a conditioned rat (top) and a control rat (bottom), covering the full-time course of the experiment. Quantitative analysis was performed on the first negative (downward)-going deflection (dot). Our previous studies of these waveforms have concentrated on this feature as it has the shortest latency, is reliably present, coincides with local evoked unit activity, shows experience-dependent plasticity, and reflects transmission from the auditory thalamus to the amygdala[7,30]. The other components of the waveform visible in these examples are not reliably present across trials and subjects, and little is known about their origin and mechanisms[7]. **b**, Fear conditioning increases the slope and amplitude of CS-EPs, but unpaired training does not. Slope and amplitude of the negative-going potential are normalized as a percentage of the mean values before training (sessions 1 and 2). The normalized slope and amplitude of the evoked potentials were evaluated statistically with two-factor ANOVAs with group (conditioned, control) as the between-subjects factor and experimental session as within-subject factor. A significant group–session interaction was observed for both measures (slope, $F(6,60) = 2.59$, $P < 0.05$; amplitude, $F(6,60) = 2.70$; $P < 0.05$). Significant differences of post hoc analyses are indicated (* Duncan, $P < 0.05$, between groups; # Duncan, $P < 0.05$, within group with respect to pretraining sessions 1 and 2). Error bars, ± s.e.m. **c**, Fear conditioning leads to associative conditioning of fear behaviour. Freezing responses during the CS and pre-CS period were evaluated statistically with two-factor ANOVAs with group (conditioned, control) as the between-subjects factor and experimental session as within-subject factor. A significant group–session interaction was observed for CS freezing ($F(6,60) = 5.23$, $P < 0.001$) but not for pre-CS freezing ($F(6,60) = 0.42$, $P > 0.1$) (not shown). Significant difference of post hoc analysis are indicated (* Duncan, $P < 0.05$, between groups). Freezing in sessions in which US presentations occur (sessions 3–5) is not useful as a measure of fear conditioning. Associative conditioning of freezing is best shown in session 6, in which only the CS was presented. The reduction in freezing in session 7 relative to session 6 reflects extinction of the CS–US association. The small amount of freezing exhibited by the control group after training (~5 s) reflects normal acquisition of freezing to the experimental context that extends into, but which is not elicited by, the CS[8,10]. Error bars, ± s.e.m.

training ($F(6, 60) = 0.42$, $P > 0.1$). Conditioned animals showed more freezing during the CS than during the pre-CS period ($F(6, 60) = 5.2$, $P > 0.01$), whereas freezing did not differ during the pre-CS and CS periods in the control group ($F(6, 60) = 0.67$, $P > 0.1$). The elevated freezing to the CS relative to the pre-CS period in the conditioned group and the equivalence of freezing in the CS and pre-CS periods for the control group leads to two conclusions. First, freezing during the CS in the control group after training is caused by the experimental context and continues into but is not evoked by the CS. Second, freezing during the CS in the conditioned group is, at least in part, specifically related to the occurrence of the CS and its association with the US.

In previous studies of freely behaving rats, changes in hippocampal field potentials measured in the course of learning have been shown to be attributable in part to modulation of brain temperature by task-related changes in locomotor activity[11,16]. Also, hippocampal field potentials are generally susceptible to modulation by behavioural state at the time of evoked potential sampling[11,17–19]. The dramatic acquisition of freezing behaviour in the course of fear conditioning therefore raises the question of whether this learning-induced change in behaviour may produce the observed changes in CS-EPs in the LA through tonic effects related to brain temperature or other behaviourally related factors that merely coincide with field-potential measurements.

Despite a greater than 10-fold increase in freezing behaviour by both groups in the course of training compared with pre-training testing, and the corresponding increase in the proportion of freezing-coincident sampling of evoked potentials during the CS (from approximately 1 of 20 freezing-coincident samples for both groups in sessions 1 and 2, to approximately 12 of 20 freezing-coincident samples for both groups in session 5), only conditioned animals showed increases in CS-EPs during training with respect to baseline levels, and only in sessions with paired training (sessions 4 and 5); control group CS-EPs showed no significant change during any session, relative to baseline testing.

These data indicate that our measures of CS-EPs are not modulated by freezing expressed at the time of field-potential sampling, or by possible behavioural modulation of brain temperature during the CS. The increases in slope and amplitude of CS-EPs measured in this experiment do not simply correlate with freezing behaviour, rather, they correlate with the presence of contingency information that identifies the CS as a danger signal, and with the degree to which the conditioned group makes use of this information after training.

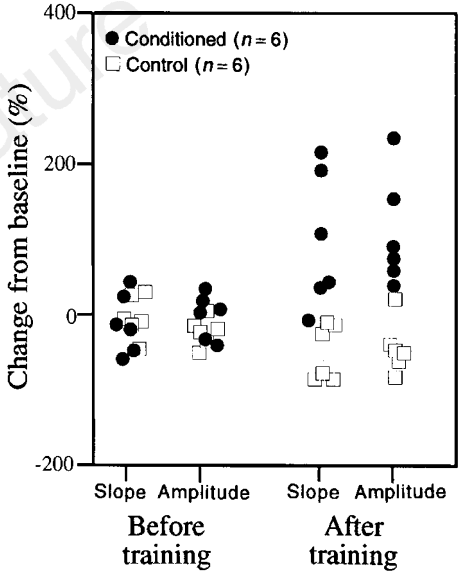

Figure 2 Scattergram of slope and amplitude values for each of the control and conditioned animals, before and after training. Pictured are normalized slope and amplitude values for each animal at the beginning of the experiment (testing, session 1), and in the first testing session after training (session 6). Points have been offset horizontally as needed to allow every point to be seen. Training had a reliable effect on the slope and amplitude of the CS-EP in the conditioned group, but not the control group.

As in our previous study of LTP and auditory evoked field potentials in the LA, the latency of CS-EPs measured in the present study varied between rats, but always fell within the latency range (15–30 ms) that invariably corresponded to histologically confirmed electrode placement within the LA[7]. The mean latency of CS-EPs across all rats (18.52 ± 3.58 ms) matched that measured in the LTP study (18.50 ± 2.65 ms), which used similar auditory stimulation parameters[7], and these latencies were not altered by either LTP induction or fear conditioning. This indicates that the potentials recorded in the two studies reflect similar stimulus-locked responses from the same general population of cells. As noted above, anatomical and physiological evidence identified these field potentials as being locally generated in the LA. Further, the coincidence of the latency of the peak negativity of the evoked potentials with the latency of single neuron activity concurrently elicited by the auditory stimulus suggested that the negative-going component of the potentials reflects extracellular currents arising from local postsynaptic activation[7]. LTP induction in anaesthetized animals produced effects of similar magnitude on both auditory evoked field potentials (change in slope over baseline, $+129.59 \pm 6.88\%$) and on electrical single-pulse stimulation (the typical test stimulus for LTP studies; change in slope over baseline, $+108.2 \pm 10.93\%$)[7]. Fear conditioning produced effects of similar magnitude on CS-EPs (change in slope over baseline, $+98.5 \pm 36.94\%$). Fear conditioning also alters single unit responses in the LA[20], and the conditioned changes in unit activity occur at latencies consistent with the changes we found in CS-EPs.

Our data indicate that CS-EPs in the LA reflect processes relevant to conditioned fear. In particular, to the extent that the negative-going slope can be interpreted as a measure of synaptic activation, we can conclude that fear conditioning, like LTP induction in CS pathways, potentiates synaptic currents. Because the same treatment potentiated both synaptic currents and conditioned fear behaviour over the same general time course, it is plausible that the enhancement of the field potentials reflects synaptic mechanisms that are responsible for the conditioning of fear behaviour. Processes mechanistically similar to LTP may therefore underlie the learning process which results from temporal association of the CS with the US, through which the CS comes to elicit conditioned fear responses.

Several previous studies have attempted to show that natural learning induces LTP-like changes in the hippocampus. In some of these studies, learning altered hippocampal physiology, but because the hippocampus is not required for the learned behaviour, the changes cannot account for learning[21,22]. Other studies have used behavioural tasks that are dependent on the hippocampus[23], but interpretation of these data is limited by the poor understanding of the flow of task-relevant information in specific synaptic circuits within the hippocampus and the contribution of these circuits to the behaviour under study[5,6]. In contrast, the well-defined and easily controlled sensory components of fear conditioning, and their tight coupling to mechanisms controlling the expression of learned fear responses, make this system well suited for such an analysis. We previously induced LTP in circuits known to be involved in fear conditioning[7] and have now shown that fear conditioning alters neural activity in these circuits in the same way as LTP induction. Furthermore, we measured both artificial LTP and fear conditioning using an auditory test stimulus, which in the fear-conditioning experiment was the environmental cue that the animals learned to fear.

Other similarities exist between fear conditioning and the classic form of hippocampal LTP, which depends on glutamatergic

mechanisms, particularly processes mediated by the NMDA (*N*-methyl-D-aspartate) receptor[1,2]. CS processing in LA involves glutamatergic transmission[24–26], and the blockade of NMDA receptors in LA and adjacent regions interferes with fear conditioning[27–29]. Also, facilitation of AMPA/NMDA receptor function modulates fear conditioning and hippocampal LTP in much the same way: both fear conditioning and LTP induction occur at an accelerated rate, but with no change in the final level of acquired conditioned fear or ceiling of potentiation[9]. Thus the LTP-like mechanisms engaged by fear conditioning may share mechanistic features with the more thoroughly studied, NMDA-dependent mechanisms known to be involved in hippocampal LTP, but which have been difficult to relate to hippocampal-dependent learning processes. It remains to be determined whether changes in synaptic strength produced in the amygdala by LTP induction and those produced by fear conditioning are both NMDA dependent. Such a demonstration would help to provide a mechanistic link between LTP and at least one form of memory. □

Methods

Surgery. Rats were anaesthetized and implanted with a stainless-steel recording electrode (0.6 mΩ) in the LA, and a ground electrode in the skull, under aseptic surgical conditions. The electrodes were mounted to the skull using dental cement. The wound was sutured and analgesics administered, and animals recovered for at least 5 days before the experiment.

Apparatus. The conditioning chamber was constructed of stainless-steel bars, acoustically transparent to the CS frequency. The chamber was kept within a ventilated and temperature-regulated acoustic isolation box lined with anechoic panels. Stimulus delivery and data acquisition were controlled by a custom-made Matlab application, using a Cambridge Electronics Devices 1401+. The isolation box was equipped with a video camera and VCR for recording of behaviour.

Conditioning protocol. The CS frequency was chosen so that the rat's head would be acoustically transparent to the CS, reducing the effect of head position on CS intensity at the tympani. The US (0.3 mA, 500 ms) was delivered through the floor of the conditioning chamber. In paired sessions, the US occurred immediately after the end of each CS. In unpaired sessions, the US occurred during the inter-CS interval (5 US per session; mean interval between CS and US, 78 s; range, 60–120 s). The sequence of testing and training sessions over 6 days is shown in Fig. 1.

Received 1 August; accepted 6 October 1997.

1. Malenka, R. C. & Nicoll, R. A. NMDA-receptor-dependent synaptic plasticity: multiple forms and mechanisms. *Trends Neurosci.* **16,** 521–527 (1993).
2. Bliss, T. V. P. & Collingridge, G. L. A synaptic model of memory: long-term potentiation in the hippocampus. *Nature* **361,** 31–39 (1993).
3. Brown, T. H. & Chattarji, S. in *Models of Neural Networks II* (eds Domany, E., Van Hemmen, J. L. & Schulten, K.) 287–314 (Springer-Verlag, New York, 1994).
4. Stäubli, U. V. in *Brain and Memory: Modulation and Mediation of Neuroplasticity* (eds McGaugh, J. L., Weinberger, N. M. & Lynch, G.) 303–318 (Oxford Univ. Press, New York, 1995).
5. Barnes, C. A. Involvement of LTP in memory: Are we "searching under the streetlight?". *Neuron* **15,** 751–754 (1955).
6. Eichenbaum, H. The LTP–memory connection. *Nature* **378,** 131–132 (1995).
7. Rogan, M. T. & LeDoux, J. E. LTP is accompanied by commensurate enhancement of auditory-evoked responses in a fear conditioning circuit. *Neuron* **15,** 127–136 (1995).
8. Phillips, R. G. & LeDoux, J. E. Differential contribution of amygdala and hippocampus to cued and contextual fear conditioning. *Behav. Neurosci.* **106,** 274–285 (1992).
9. Rogan, M. T., Stäubli, U. V. & LeDoux, J. E. AMPA-receptor facilitation accelerates fear learning without altering the level of conditioned fear acquired. *J. Neurosci.* **17,** 5928–5935 (1997).
10. Kim, J. J. & Fanselow, M. S. Modality-specific retrograde amnesia of fear. *Science* **256,** 675–677 (1992).
11. Moser, E. I., Moser, M.-B. & Andersen, P. Potentiation of dentate synapses initiated by exploratory learning in rats: dissociation from brain temperature, motor activity, and arousal. *Learn. Memory* **1,** 55–73 (1994).
12. Blanchard, R. J. & Blanchard, D. C. Passive and active reactions to fear-eliciting stimuli. *J. Comp. Physiol. Psychol.* **68,** 129–135 (1969).
13. Blanchard, R. J. & Blanchard, D. C. Crouching as an index of fear. *J. Comp. Physiol. Psychol.* **67,** 370–375 (1969).
14. Bouton, M. E. & Bolles, R. C. Conditioned fear assessed by freezing and by the suppression of three different baselines. *Anim. Learn. Behav.* **8,** 429–434 (1980).
15. Bolles, R. C. & Fanselow, M. S. A perceptual-defensive-recuperative model of fear and pain. *Behav. Brain Sci.* **3,** 291–323 (1980).
16. Moser, E., Mathiesen, I. & Anderson, P. Association between brain temperature and dentate field potentials in exploring and swimming rats. *Science* **259,** 1324–1326 (1993).
17. Winson, J. & Absug, C. Neuronal transmission through hippocampal pathways dependent on behavior. *J. Neurophysiol.* **41,** 716–732 (1978).
18. Leung, S. Behavior-dependent evoked potentials in the hippocampal CA1 region of the rat. I. Correlation with behavior and EEG. *Brain Res.* **198,** 95–117 (1980).
19. Buzsaki, G., Grastyan, E., Czopf, J., Kellenyi, L. & Prohaska, O. Changes in neuronal transmission in the rat hippocampus during behavior. *Brain Res.* **225,** 235–247 (1981).
20. Quirk, G. J., Repa, J. C. & LeDoux, J. E. Fear conditioning enhances short-latency auditory responses of lateral amygdala neurons: parallel recordings in the freely behaving rat. *Neuron* **15,** 1029–1039 (1995).
21. Skelton, R. W., Scarth, A. S., Wilkie, D. M., Miller, J. J. & Philips, G. Long-term increases in dentate granule cell responsivity accompany operant conditioning. *J. Neurosci.* **7,** 3081–3087 (1987).
22. Deadwyler, S. A., West, M. O., Christian, E., Hampson, R. E. & Foster, T. C. Sequence-related changes in sensory-evoked potentials in the dentate gyrus: as mechanism for item-specific short-term information storage in the hippocampus. *Behav. Neural Biol.* **44,** 201–212 (1985).
23. Jeffrey, K. J. LTP and spatial learning—where to next? *Hippocampus* **7,** 95–110 (1997).
24. Farb, C. R. & LeDoux, J. E. NMDA and AMPA receptors in the lateral nucleus of the amygdala are postsynaptic to auditory thalamic afferents. *Synapse* **27,** 106–121 (1997).
25. Li, X., Phillips, R. G. & LeDoux, J. E. NMDA and non-NMDA receptors contribute to synaptic transmission between the medial geniculate body and the lateral nucleus of the amygdala. *Exp. Brain Res.* **105,** 87–100 (1995).
26. Li, X. F., Stutzmann, G. E. & LeDoux, J. L. Convergent but temporally separated inputs to lateral amygdala neurons from the auditory thalamus and auditory cortex use different postsynaptic receptors: *in vivo* intracellular and extracellular recordings in fear conditioning pathways. *Learn. Memory* **3,** 229–242 (1996).
27. Miserendino, M. J. D., Sananes, C. B., Melia, K. R. & Davis, M. Blocking of acquisition but not expression of conditioned fear-potentiated startle by NMDA antagonists in the amygdala. *Nature* **345,** 716–718 (1990).
28. Maren, S., Aharonov, G., Stote, D. L. & Fanselow, M. S. N-Methyl-d-Aspartate receptors in the basolateral amygdala are required for both acquisition and expression of the conditional fear in rats. *Behav. Neurosci.* **110,** 1365–1374 (1996).
29. Gewirtz, J. C. & Davis, M. Second-order fear conditioning prevented by blocking NMDA receptors in amygdala. *Nature* **388,** 471–473 (1997).
30. Rogan, M. T. & LeDoux, J. E. Intra-amygdala infusion of APV blocks both auditory evoked potentials in the lateral amygdala and thalamo-amygdala transmission, but spares cortico-amygdala transmission. *Soc. Neurosci. Abstr.* **21,** 1930 (1995).

Acknowledgements. We thank D. Ringach for software development and M. Hou for histology and help with the surgical preparation of subjects.

Correspondence and requests for materials should be addressed to M.T.R. (e-mail: rogan@cns.nyu.edu).

Fear conditioning induces a lasting potentiation of synaptic currents *in vitro*

M. G. McKernan & P. Shinnick-Gallagher

Department of Pharmacology and Toxicology, The University of Texas Medical Branch, Galveston, Texas 77555-1031, USA

The amygdala plays a critical role in the mediation of emotional responses, particularly fear, in both humans and animals[1–4]. Fear conditioning, a conditioned learning paradigm, has served as a model for emotional learning in animals, and the neuroanatomical circuitry underlying the auditory fear-conditioning paradigm is well characterized[5]. Synaptic transmission in the medial geniculate nucleus (MGN) to lateral nucleus of the amygdala (LA) pathway, a key segment of the auditory fear conditioning circuit, is mediated largely through *N*-methyl-D-aspartate (NMDA) and non-NMDA (such as α-amino-3-hydroxy-5-methyl-4-isoxazolepropionic acid (AMPA)) glutamate receptors[6]; the potential for neural plasticity in this pathway is suggested by its capacity to support long-term potentiation (LTP)[7,8]. Here we report a long-lasting increase in the synaptic efficacy of the MGN–LA pathway attributable to fear-conditioning itself, rather than an electrically induced model of learning. Fear-conditioned animals show a presynaptic facilitation of AMPA-receptor-mediated transmission, directly measured *in vitro* with whole-cell recordings in lateral amygdala neurons. These findings represent one of the first *in vitro* measures of synaptic plasticity resulting from emotional learning by whole animals.

Fear-conditioned rats, when exposed to a tone (conditioned stimulus, CS) repeatedly paired with an aversive footshock (unconditioned stimulus, US), respond with a potentiated acoustic startle reflex (+58.9% ± 11.6%, $n = 27$; see Methods) immediately following CS presentation, whereas unpaired control rats, exposed to the CS and US in an unpaired, pseudorandom fashion, do not (+2.6% ± 5.6%, $n = 23$; unpaired *t*-test: $P < 0.0001$) (Fig. 1a). *In vivo* experiments suggest that the amygdala is involved in both the acquisition and expression of fear-potentiated startle[9–11]. We prepared coronal slices from fear-conditioned rats 24 hours after